X-RAY EMISSION FROM YOUNG BROWN DWARFS IN THE ORION NEBULA CLUSTER

Thomas Preibisch,[1] Mark J. McCaughrean,[2,3] Nicolas Grosso,[4] Eric D. Feigelson,[5]
Ettore Flaccomio,[6] Konstantin Getman,[5] Lynne A. Hillenbrand,[7] Gwendolyn Meeus,[3]
Giusi Micela,[6] Salvatore Sciortino,[6] and Beate Stelzer[6,8]

ABSTRACT

We use the sensitive X-ray data from the *Chandra* Orion Ultradeep Project (COUP) to study the X-ray properties of 34 spectroscopically identified brown dwarfs with near-infrared spectral types between M6 and M9 in the core of the Orion Nebula Cluster. Nine of the 34 objects are clearly detected as X-ray sources. The apparently low detection rate is in many cases related to the substantial extinction of these brown dwarfs; considering only the brown dwarfs with $A_V \leq 5$ mag, nearly half of the objects (7 out of 16) are detected in X-rays. Our 10 day long X-ray light curves of these objects exhibit strong variability, including numerous flares. While one of the objects was only detected during a short flare, a statistical analysis of the light curves provides evidence for continuous ("quiescent") emission in addition to flares for all other objects. Of these, the $\sim$M9 brown dwarf COUP 1255 (=HC 212) is one of the coolest known objects with a clear detection of quiescent X-ray emission. The X-ray properties (spectra, fractional X-ray luminosities, flare rates) of these young brown dwarfs are similar to those of the low-mass stars in the Orion Nebula Cluster, and thus there is no evidence for changes in the magnetic activity around the stellar/substellar boundary, which lies at $\sim$M6 for Orion Nebula Cluster sources. Since the X-ray properties of the young brown dwarfs are also similar to those of M6–M9 field stars, the key to the magnetic activity in very cool objects seems to be the effective temperature, which determines the degree of ionization in the atmosphere.

Subject headings: open clusters and associations: individual (Orion Nebula Cluster) — stars: activity —
stars: low-mass, brown dwarfs — stars: pre–main-sequence — X-rays: stars

1. INTRODUCTION

Brown dwarfs (BDs) are objects with masses below $\sim 0.075\ M_\odot$, the stellar/substellar boundary (see Basri 2000 for a review). In contrast to stars, which derive their luminosity from hydrogen fusion, BDs never reach sufficiently high core temperatures to start hydrogen burning, though brief episodes of deuterium and lithium burning occur early in their evolution. With no sustainable internal fusion energy source, BDs continuously cool down and dim with time. During the first few Myr of their evolution, BDs are thus warmer and orders of magnitude brighter than at older ages: for example, between the ages of 1 Myr and 5 Gyr, a 0.03 $M_\odot$ BD cools from $T_{\rm eff} = 2660$ K down to $T_{\rm eff} = 600$ K, and its luminosity drops by 4 orders of magnitude from $\log (L_*/L_\odot) = -2.1$ to $\log (L_*/L_\odot) = -6.1$ (Baraffe et al. 1998). Young BDs can thus be readily detected at larger distances much more easily than older BDs, and as a consequence, numerous young BDs have recently been discovered in several nearby star-forming regions. The largest population is found in the Orion Nebula Cluster (ONC;

McCaughrean et al. 1995; Hillenbrand & Carpenter 2000; Muench et al. 2002).

Even when young, BDs are relatively cool and dim objects, and one would not intuitively expect them to emit high-energy radiation. Also, as BDs have a fully convective internal structure, they cannot possess a solar-like $\alpha - \Omega$ dynamo, which is thought to be the energy source of X-ray activity in late-type stars. Nevertheless, some brown dwarfs have been detected as X-ray sources (§ 2). The nature of the X-ray emission from BDs (and similarly from fully convective very-low mass stars) and the origin of their activity is still not well understood.

In this paper, we focus on a relatively small sample of spectroscopically confirmed BDs in the ONC classified by Slesnick et al. (2004, hereafter SHC04) and their X-ray properties as measured in the *Chandra* Orion Ultradeep Project (COUP).[9] A significantly larger sample of candidate BDs has been identified in the ONC by several authors based on broadband optical and near-infrared photometry, but their status as true BDs remains unconfirmed by spectroscopy. In a subsequent paper, we will present an analysis of the X-ray properties of the larger sample of very low mass stars and BD candidates in the region as detected in deep near-infrared imaging photometry obtained with the ESO Very Large Telescope and characterized in terms of their photometric properties alone (M. J. McCaughrean et al. 2005, in preparation).

2. PREVIOUS X-RAY DETECTIONS OF SPECTROSCOPICALLY CONFIRMED BROWN DWARFS

The first (and at that time unrecognized) detection of X-ray emission from a BD was made as early as 1991, when *ROSAT* obtained a deep X-ray image of the Chamaeleon star-forming

[1] Max-Planck-Institut für Radioastronomie, Auf dem Hügel 69, D-53121 Bonn, Germany.
[2] School of Physics, University of Exeter, Stocker Road, Exeter EX4 4QL, Devon, UK.
[3] Astrophysikalisches Institut Potsdam, An der Sternwarte 16, D-14482 Potsdam, Germany.
[4] Laboratoire d'Astrophysique de Grenoble, Université Joseph-Fourier, F-38041 Grenoble cedex 9, France.
[5] Department of Astronomy and Astrophysics, Pennsylvania State University, University Park, PA 16802.
[6] INAF, Osservatorio Astronomico di Palermo G. S. Vaiana, Piazza del Parlamento 1, I-90134 Palermo, Italy.
[7] Department of Astronomy, California Institute of Technology, Mail Code 105-24, Pasadena, CA 91125.
[8] Dipartimento di Scienze Fisiche ed Astronomiche, Università di Palermo, Piazza del Parlamento 1, I-90134 Palermo, Italy.

[9] Links to the COUP data set are available in the electronic edition of the *Supplement*.

region. One of the weak X-ray sources was identified with a faint ($V \sim 21$ mag) point source, for which no further information was available at the time. Several years later, after the first confirmed BDs were announced in 1995, Neuhäuser & Comerón (1998) presented an optical spectrum of this object, Cha Hα 1, and derived a spectral type of M7.5, from which they inferred a substellar mass of $\sim 0.05\ M_\odot$. This episode serves to demonstrate that the main obstacle in the investigation of X-ray emission from BDs is often not their detection as faint X-ray sources, but rather the lack of optical/near-infrared spectroscopy necessary for reliable mass estimates.

Although some further BD detections were made with *ROSAT* (e.g., Comerón et al. 2000), the X-ray fluxes were only marginally above the detection limits, and the $\sim 15''$ spatial resolution of the satellite often led to identification difficulties. The advent of the new X-ray observatories *XMM-Newton* and *Chandra* boosted the effort with their greatly increased sensitivity and, in the case of *Chandra*, superb spatial resolution ($\sim 1''$). For example, X-rays were detected from two BDs in the ρ Oph star-forming region by both satellites and showed strong long-term variability (Imanishi et al. 2001; Ozawa et al. 2005). A *Chandra* observation of the young cluster IC 348 provided X-ray detections of 7 very low mass objects, 4 of which are spectroscopically confirmed BDs (Preibisch & Zinnecker 2001, 2002). Tsuboi et al. (2003) resolved X-rays from the ~ 10 Myr old M8.5–M9 BD TWA-5B separated by $2''$ from its primary, TWA-5A, in the nearby TW Hya association, while Gizis & Bharat (2004) saw no emission from 2MASS J1207334−393254, another M8 BD in the same association. The former was detected in quiescence at a level of $\log L_X = 27.6$ ergs s^{-1} and $\log (L_X/L_{bol}) = -3.4$ with an unusually soft spectrum, while for the latter, upper limits of $\log L_X < 26.1$ ergs s^{-1} and $\log (L_X/L_{bol}) < -4.8$ were determined. Finally, in the Chamaeleon I cloud, Feigelson & Lawson (2004) reported X-rays from three objects around the substellar limit in the northern molecular core using *Chandra*, while Stelzer et al. (2004) detected two spectroscopically confirmed BDs and several BD candidates in the southern core using *XMM-Newton*.

To date, just two older field BDs have been detected in X-rays. The first of these is the nearby ($d = 5$ pc) M9 dwarf LP 944-20, with an estimated mass of $\sim 0.06\ M_\odot$ and age of ~ 600 Myr. Rutledge et al. (2000) discovered an X-ray flare from LP 944-20 during a *Chandra* observation but detected no quiescent emission. At the flare peak, the X-ray luminosity was $\log L_X = 26.1$ ergs s^{-1} and $\log (L_X/L_{bol}) \sim -3.7$. A subsequent deep *XMM-Newton* observation by Martín & Bouy (2002) provided a very sensitive upper limit of $\log L_X < 23.5$ ergs s^{-1} and $\log (L_X/L_{bol}) < -6.3$ for possible quiescent emission. A powerful X-ray flare and probable quiescent emission,[10] was detected from the second field source, the M8.5+M9 binary Gl 569 Ba, Bb, which orbits the nearby ($d = 10$ pc), ~ 300–800 Myr old M2 star Gl 569 A with $5''$ separation (Stelzer 2004). A dynamical mass determination for the components in the $0''.1$ binary Ba, Bb gives $M_{Ba} = 0.055$–$0.087\ M_\odot$ and $M_{Bb} = 0.034$–$0.070\ M_\odot$ (99% confidence intervals; Zapatero Osorio et al. 2004); the lower mass component at least is the first model-independently confirmed substellar object.

3. X-RAY–EMITTING BROWN DWARFS IN THE ONC

3.1. *Previous X-Ray Results on Very Low Mass Objects in the ONC*

Prior to COUP, the ONC had been observed with both imaging instruments, ACIS and HRC, on board *Chandra*. The results

---

[10] The quiescent emission was only seen after, but not before the flare, and thus may be an afterglow of the flare.

of two ACIS-I observations with a combined exposure time of 23 hr were reported in Garmire et al. (2000) and Feigelson et al. (2002a, 2002b, 2003). These ACIS observations revealed X-ray detections of about 30 very low mass objects (Feigelson et al. 2002a); for most of these objects, however, no optical/infrared spectra were available and it was therefore unclear whether they were BDs or low-mass stars. Several of the very low mass objects showed X-ray flares, which appeared to be similar in frequency and morphology to the flares on low-mass stars. Feigelson et al. (2002a) concluded that the candidate very low mass objects had X-ray properties similar to those of low-mass stars and that magnetic activity appears to decline as the very low mass objects evolve. Flaccomio et al. (2003a, 2003b) presented an analysis of their 17.5 hr HRC-I observation of the ONC. From a ''composite source analysis'' of a sample of very low mass objects (1 X-ray–detected object and 14 upper limits), they concluded that the BDs seem to follow the same $L_X \leftrightarrow M$ relationship as low-mass stars.

3.2. *The ONC Brown Dwarf Sample*

The presence of an extensive substellar population in the ONC has been deduced in a series of studies (e.g., McCaughrean et al. 1995; Hillenbrand & Carpenter 2000; Luhman et al. 2000; Lucas & Roche 2000; Muench et al. 2002). These studies, however, were generally based on photometry alone, which can lead to ambiguities when trying to establish the membership and mass of a specific source, as opposed to the properties of the ensemble population. To derive more definitive properties for a subset of sources, SHC04 recently presented a spectroscopic study of candidate BD members in the central $5'.1 \times 5'.1$ ($\sim 0.7 \times 0.7$ pc) part of the ONC. Using near-infrared and optical spectra, they derived spectral types and basic parameters, such as bolometric luminosity and extinction, for about 100 faint objects, from which they then constructed an H-R diagram. Masses were inferred using the D'Antona & Mazzitelli (1997) evolutionary tracks, leading to the identification of 34 objects with masses nominally below $0.075\ M_\odot$.

It should be noted that the majority of the SHC04 spectral classifications were based on near-infrared spectra, as less than half of the sources in their sample had corresponding optical spectra. Conversely, a small handful of sources had *only* optical spectra, which were then used for their classification. At issue here is the well-known fact that near-infrared classification tends to yield systematically later spectral types for young brown dwarfs than given by optical spectral classification (see, e.g., Luhman & Rieke 1999; Luhman et al. 2003). Typically, there is a shift to later types by ~ 1 subclass for M6–M7 sources, and by ~ 1–2 subclasses for types at M8 and later. This systematic shift can be seen in the ONC sources of SHC04 for which both near-infrared and optical spectra were available (their Tables 1 and 2).

Another important point to note is that these very young objects should have relatively low surface gravities, which can lead to significant changes in the depth of some of the traditional classification indices; e.g., those based on the near-infrared water absorption features, in turn causing errors in the resulting spectral types, effective temperatures, and placement in the H-R diagram (see, e.g., McGovern et al. 2004; Gorlova et al. 2003; Lucas et al. 2001; Wilking et al. 2004). SHC04 addressed the spectral typing issue by measuring standards drawn from a range of high surface gravity main-sequence stars, low surface gravity sources from relatively young clusters, and field giants. However, when converting from spectral types to effective temperatures, they used a high-gravity dwarf temperature scale,
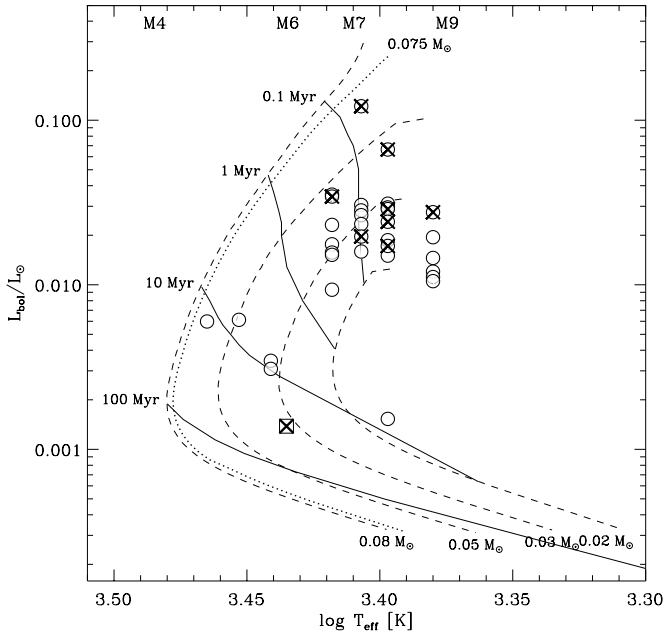
Fig. 1.—H-R diagram for the spectroscopically confirmed ONC BDs (*circles*) from SHC04. HC 722, which is the only object for which the spectral analysis suggested a high surface gravity (rather than the low gravity expected for very young BDs), is plotted as a square. Objects detected as X-ray sources in the COUP data are marked by crosses. The evolutionary tracks (*dotted lines*) and isochrones (*solid lines*) are from D'Antona & Mazzitelli (1997).

pointing out that young pre–main-sequence objects appear observationally closer to dwarfs than giants or subgiants and also that no accurate temperature or bolometric correction scales for pre–main-sequence stars are available to date.

By contrast, other authors (e.g., White et al. 1999; Luhman et al. 2003) have used a spectral type to effective temperature conversion based on optical spectral types and fitting the isochrones of Baraffe et al. (1998) for young brown dwarfs. They suggest that for a given optical M spectral type, young objects have effective temperatures ∼100–200 K warmer than field dwarfs. This compounds the near-infrared/optical shift in spectral type. For example, consider a young source with an optical spectral type of M7 and, for the sake of argument, an M8 spectral type derived from a near-infrared spectrum. The field dwarf temperature scale adopted by SHC04 gives ∼2500 K for spectral type M8, and ∼2620 K for M7. The pre–main-sequence temperature scales of White et al. (1999) and Luhman et al. (2003) give ∼2850 K as the effective temperature for the optical spectral type M7. Thus, in this hypothetical example, the near-infrared classification and field dwarf temperature scale would yield an effective temperature of 2500 K for the source, where the optical classification and PMS temperature scale would give 2850 K. From Figure 1, it can be seen that such a temperature shift would result in an upward revision of the mass of the source by a factor of 2–3 using the D'Antona & Mazzitelli (1997) tracks.

A further problem is that there is substantial detailed disagreement between various pre–main-sequence evolutionary tracks covering the stellar/substellar transition at early ages (e.g., those of D'Antona & Mazzitelli 1997 as used by SHC04 vs. the models of Baraffe et al. 1998 or Siess et al. 2000 used elsewhere; see, e.g., the analyses of Luhman 1999 and Hillenbrand & White 2004). In particular, Hillenbrand & White (2004) concluded that none of the currently available sets of evolutionary models provide a fully satisfactory match between masses de-

rived on the basis of pre–main-sequence tracks and those measured dynamically: there is a general trend that they underpredict mass by 10%–30% in the range 1.2–0.3 $M_\odot$, the lowest masses presently testable in this manner.

These issues are too involved to be analyzed in detail here. Furthermore, it is not practical to rederive the spectral types, effective temperatures, and masses for the SHC04 sample here. For example, roughly 75% of the 34 sources classified as BDs by SHC04 do not have optical spectra and thus near-infrared spectral types must be used. As a consequence, it is possible that some of the 34 sources that SHC04 spectroscopically classified as BDs do in fact have stellar masses, but we shall assume for present purposes that all of them are indeed true BDs. We focus on the nominal BD sources exclusively, omitting the objects in the SHC04 sample with masses nominally in the stellar regime. These, and the numerous additional BD candidates seen in near-infrared images, will be treated in a separate paper.

Finally, we note that the latest spectral type found by SHC04 was L0, for the source HC 722. As this source was also detected in the COUP data during a flare (COUP 344) as discussed below, it would have represented the latest spectral type source seen in X-rays to date. However, a careful reassessment of the SHC04 optical spectrum for HC 722 (see erratum of SHC04) has shown that its spectral type is in fact significantly earlier, at around M6–M6.5. We adopt this revised spectral type in the remainder of our analysis, along with the corresponding new physical parameters $\log T_{\rm eff} = 3.435$, $\log (L_{\rm bol}/L_\odot) = -2.88$, and a mass of 0.035 $M_\odot$. It is also important to note that HC 722 was the only COUP-detected BD candidate showing indications of a high surface gravity, suggesting that it may in fact be a foreground field star. This possibility is discussed in more detail in § 4.2.

3.3. *The COUP Observation*

The COUP observation of the ONC is the longest and deepest X-ray observation ever made of a young stellar cluster, providing a rich and unique data set for a wide range of science studies. Full observational details, a complete description of the data analysis, and the definitions of the derived X-ray quantities can be found in Getman et al. (2005a). Briefly, the total exposure time of the COUP image with ACIS-I on *Chandra* was 838,100 s (232.8 hr or 9.7 days) with a single $17' \times 17'$ FOV pointing centered near the Trapezium stars. A total of 1616 individual X-ray sources were found in the COUP image, and the superb PSF and the high accuracy of the aspect solution allowed a clear and unambiguous identification of ≃1400 X-ray sources with near-infrared or optical counterparts, with median offsets of just 0″15 and 0″24, respectively (Getman et al. 2005b). The X-ray luminosities of the sources were determined in the spectral fitting analysis; integrating the best-fit model source flux over the [0.5–8.0] keV band yielded the intrinsic (extinction-corrected) X-ray luminosity ($L_{\rm X} \equiv L_{t,c}$ in the nomenclature of Getman et al. 2005a). The detection limit of the COUP data is $\log L_{\rm X} = 27.3$ ergs s^{-1} for lightly absorbed sources. Given the typical bolometric luminosities of young BDs in the ONC of 10^{-1}–10^{-3} $L_\odot$, we are thus able to probe the X-ray activity of these objects down to levels of $L_{\rm X}/L_{\rm bol} \sim 10^{-5}$–$10^{-3}$.

3.4. *X-Ray–detected BDs in COUP*

Nine of the 34 spectroscopic BDs (objects with mass estimates <0.075 $M_\odot$) in the SHC04 sample are detected as X-ray sources in the COUP data set, and the observed X-ray properties of these objects are discussed in detail below. A summary of

TABLE 1
X-Ray−detected Brown Dwarfs in the ONC: Near-infrared Properties

	VLT					Keck				
COUP Number (1)	Number (2)	θ (arcsec) (3)	J (mag) (4)	H (mag) (5)	K_s (mag) (6)	HC Number (7)	A_V (mag) (8)	Spectral Type (9)	M ($M_\odot$) (10)	$\log(L_{bol})$ ($L_\odot$) (11)
280............................	133	0.29	16.27	15.24	14.50	64	4.46	M7–M9	0.03	−1.617
344............................	201	0.27	17.10	16.58	16.12	722	0.00	M6–M6.5	0.03	−2.880
371............................	225	0.25	15.06	13.90	13.04	90	6.77	M7.5	0.07	−0.915
764............................	558	0.10	16.25	15.57	14.91	565	5.60	M8	0.02	−1.764
941............................	724	0.03	16.35	15.45	14.75	594	2.20	M7.5	0.03	−1.707
1125..........................	880	0.14	14.53	13.72	13.22	22	1.78	M8	0.05	−1.178
1194..........................	934	0.16	16.58	15.12	14.38	55	1.90	M8	0.03	−1.540
1255..........................	999	0.10	15.58	14.82	14.17	212	3.41	M9	0.03	−1.559
1313[a]	1055	0.14	15.14	14.45	13.94	114	1.44	M7	0.05	−1.464

Notes.—Cols. (1)–(6) are from Getman et al. (2005a) with near-infrared data in the 2MASS photometric system from the VLT unified catalog of the central $7' \times 7'$ by M. J. McCaughrean et al. (2005, in preparation); θ is the angular offset between the COUP and VLT positions for each source. Cols. (7)–(11) are from SHC04.

[a] COUP 1313 has an optical counterpart in Herbst et al. (2002), 10626 with $\langle V \rangle = 18.48$ and variability range $\Delta V = 0.39$.

their optical/near-infrared properties is given in Table 1, while their X-ray properties are listed in Table 2. For the 25 spectroscopic BDs not detected as X-ray sources, upper limits to their X-ray count rates were derived as described in the next subsection. In Figure 1, we show an H-R diagram with the all the spectroscopic BDs in the SHC04 sample. It is clear that the COUP detection likelihood is a strong function of the bolometric luminosity; this reflects the correlation between X-ray and bolometric luminosity (see below). Another factor limiting our ability to detect X-ray emission from the BDs is their extinction, as will be discussed in § 3.6.

Two aspects should be noted with respect to the derived X-ray luminosities of the BDs. First, it should be kept in mind that since the X-ray luminosities were determined from the fits to the temporally averaged spectra obtained over the full ~10 day COUP exposure, the values for the X-ray luminosities are also temporal averages over the same period. During the flares seen in the individual light curves, the luminosities can be

considerably higher. In § 4.1, we also determine the "characteristic" values of the X-ray luminosities, which can be thought of as the typical or quiescent level of X-ray energy output of these sources excluding flares. The only exception is COUP 344 (HC 722), which was only detected during a flare; for this object we estimated the flare luminosity and an upper limit to the X-ray luminosity outside the flare period (see § 4.2).

Second, since the number of source photons per spectrum is rather small (<100), the reliability of the extinction-corrected values for the X-ray luminosities, $L_{t,c}$, is not immediately clear. We have therefore compared the values for the absorbing hydrogen column density found in the spectral fits to those expected from the visual extinction according to the relation $N_H = A_V \times 1.6 \times 10^{21}$ cm^{-2} (Vuong et al. 2003), where A_V is that determined by SHC04 from their optical and near-infrared spectra. In all cases, the N_H-values found in the X-ray spectral fits are either consistent with or somewhat lower than the estimate based on A_V. This implies that our X-ray luminosities are

TABLE 2
X-Ray−detected Brown Dwarfs in the ONC: X-Ray Properties

COUP Number (1)	IAU Number (2)	NetCts (3)	$\log P_{KS}$ (4)	BB (5)	Max./Min. (6)	$\langle E \rangle$ (keV) (7)	$\log L_t$ (ergs s^{-1}) (8)	$\log L_{t,c}$ (ergs s^{-1}) (9)	$\log L_X/L_{bol}$ (10)
280................................	053507.0−052500	49	−0.7	1	1	1.2	28.2	28.7	−3.3
344 f[a]	053509.7−052406	8	−1.0	1	1	1.1	28.7	28.7	−2.0
344 q[a]	053509.7−052406	<5	...	...	...	...	<27.1	<27.1	<−3.6
371................................	053510.3−052451	63	−0.9	1	1	1.4	27.6	28.8	−3.9
764................................	053516.0−052153	65	−4.0	3	22	1.2	28.1	28.1	−3.8
941................................	053518.0−052141	43	−4.0	2	8	1.6	28.0	28.1	−3.8
1125[b]	053520.9−052534	26	−1.0	1	1	1.4	28.2	28.3	−4.2
1194..............................	053522.1−052507	24	−0.4	1	1	1.6	27.9	28.0	−4.1
1255..............................	053523.5−052350	46	−3.7	2	3	1.6	28.1	28.3	−3.8
1313..............................	053525.0−052438	94	−2.0	3	7	1.2	28.3	28.4	−3.7

Notes.—Cols. (1)–(6) and (8)–(9) are from Getman et al. (2005a), while cols. (7) and (10) are calculated here. Col. (3): Net (i.e., background-subtracted) number of X-ray photons detected. Col. (4): Logarithm of the nonparametric one-sample Kolmogorov-Smirnov (KS) test significance for the null hypothesis of a constant source. Col. (5): Number of segments into which the light curve was segmented by the Bayesian block (BB) parametric model. Col. (6): Ratio of the count rates in the highest and lowest segment Col. (7): Median energy of the detected photons for each source. Col. (8): Observed X-ray luminosity integrated over the [0.5−8.0] keV band. Col. (9): Extinction-corrected [0.5−8.0] keV band luminosity. Col. (10): Ratio of total X-ray luminosity to stellar bolometric luminosity.

[a] COUP 344 (HC 722) has two entries in this table: 344 f lists the X-ray properties during the flare, while 344 q lists the upper limits for the periods outside the flare.

[b] COUP 1125 lies on an ACIS chip gap with an effective exposure of only 364 ks.

TABLE 3
Upper Limits for the COUP Undetected Brown Dwarfs from SHC04

HC00 (1)	LC (2)	Exposure (s) (3)	A_V (4)	CF (5)	CF_c (6)	$\log L_t$ (7)	$\log L_{t,c}$ (8)	$\log (L_X/L_{bol})$ (9)
20	6	424	3.77	0.65	1.9	<27.3	<27.8	<−4.3
62	4	837	5.85	0.71	2.9	<26.9	<27.5	<−4.1
70	6	641	9.48	0.79	4.1	<27.3	<28.0	<−3.7
111	4	838	8.61	0.77	3.6	<27.0	<27.6	<−4.1
123	6	834	7.89	0.75	3.4	<27.1	<27.8	<−4.3
167	20	823	9.19	0.79	4.0	<27.7	<28.4	<−3.6
210	9	834	4.81	0.66	2.2	<27.2	<27.8	<−4.2
221	16	331	4.43	0.65	2.1	<27.9	<28.4	<−3.6
365	18	797	8.23	0.76	3.8	<27.6	<28.3	<−3.5
372	25	831	2.04	0.60	1.1	<27.6	<27.9	<−4.0
400	9	777	2.16	0.60	1.1	<27.2	<27.5	<−4.1
403	5	733	6.78	0.71	2.9	<27.1	<27.7	<−4.2
429	8	825	5.53	0.68	2.4	<27.2	<27.8	<−4.0
433	5	770	10.44	0.81	4.4	<27.1	<27.8	<−3.9
515	9	834	23.29	1.20	13.0	<27.5	<28.5	<−3.6
529	14	833	25.18	1.20	14.3	<27.7	<28.8	<−3.3
559	28	831	0.00	0.61	0.6	<27.7	<27.7	<−4.2
709	4	431	2.11	0.60	1.1	<27.1	<27.4	<−4.0
724	9	779	0.00	0.61	0.6	<27.2	<27.2	<−3.8
725	4	753	9.40	0.79	4.0	<27.0	<27.7	<−3.8
728	8	365	5.91	0.70	2.7	<27.6	<28.2	<−3.2
729	13	821	14.73	0.96	7.0	<27.6	<28.4	<−3.3
743	4	785	5.61	0.68	2.5	<26.9	<27.5	<−3.6
749	7	785	3.10	0.60	1.4	<27.1	<27.5	<−3.3
764	7	316	7.06	0.73	3.1	<27.6	<28.2	<−3.8

Notes.—Col. (1): Source number from Hillenbrand & Carpenter (2000). Col. (2): Limiting number of counts from COUP image (see text). Col. (3): COUP effective exposure time in ks. Col. (4): Visual absorption from SHC04. Col. (5): Conversion factor from count rate to flux in units of 10^{-14} ergs s^{-1} cm^{-2} (counts ks^{-1})$^{-1}$ as observed (see text). Col. (6): Conversion factor corrected for absorption. Col. (7): Total [0.5–8] keV band luminosity as observed. Col. (8): Total band luminosity corrected for absorption. Col. (9): Upper limit on $\log (L_X/L_{bol})$.

reliable and not affected by potential problems due to overestimates of the absorbing hydrogen column density in the X-ray spectral fits.

3.5. Determination of Upper Limits for the Undetected BDs

While the COUP data are generally sensitive to stars with luminosities above $\log L_X(\lim) \simeq 27.0–27.5$ ergs s^{-1} for lightly absorbed stars (Getman et al. 2005a), individual X-ray upper limits can be obtained for undetected ONC members when an estimate of the absorption is available. In Table 3, we give COUP X-ray upper limits for those 25 BDs from SHC04 that were undetected in COUP, where these upper limits were obtained from the COUP image as follows. Photons were extracted at the position of each star using the acis_extract procedure described in Getman et al. (2005a). This procedure subtracts a local background from a region containing ≃90% of the expected events based on the shape of the *Chandra* point spread function at that location in the field. Column (2) of Table 3 gives the Poissonian 68% upper confidence level of source counts based on the extracted and background counts, but truncated at 4 counts as a realistic lower limit. The table then provides COUP effective exposure times, which include telescope vignetting and other instrumental effects, and visual absorption estimates from the spectroscopy by SHC04. Conversion factors from ACIS-I count rates to X-ray fluxes are given for the observed emission (col. [5]) and intrinsic emission corrected for absorption (col. [6]). We have used the PIMMS software developed by the NASA High Energy Astrophysics
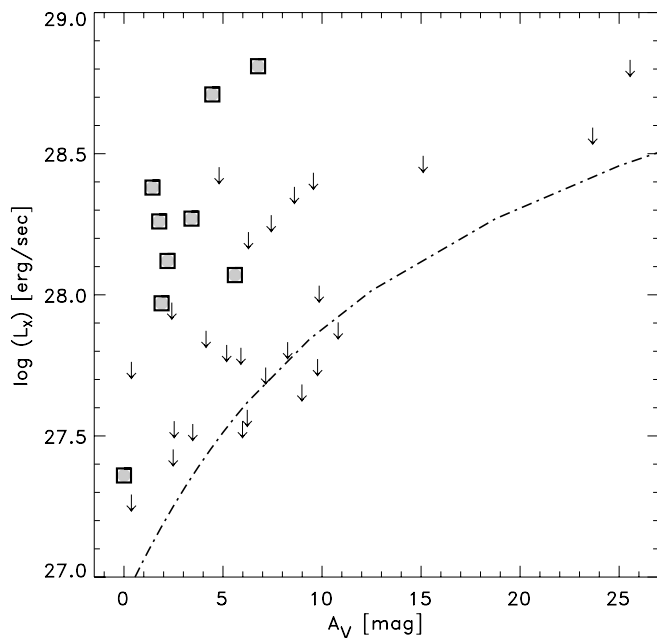

Fig. 2.—X-ray luminosities (extinction-corrected average values during the period of the COUP observation) vs. optical extinction of the BDs from SHC04. The gray filled boxes show the X-ray luminosities for the detected BDs, the arrows mark the upper limits for undetected BDs. The dot-dashed line shows the theoretical COUP sensitivity limit for detections with 5 source counts.

Science Archive Science Center, with an assumed intrinsic source spectrum of a 1 keV thermal plasma with a metal abundance of 0.4 times solar, typical for faint ONC X-ray sources (Getman et al. 2005a). The final table columns give the resulting observed and intrinsic X-ray luminosity limits assuming a distance of 450 pc to the ONC.

3.6. *Detection Fraction*

Why are only 9 of the 34 (26%) spectroscopically confirmed BDs detected in the COUP data? This low detection fraction is related not only to the intrinsic faintness of the BDs, but also to their extinction, since the X-ray detection limit increases as a function of the extinction. Many of the BDs in the SHC04 sample suffer from substantial extinction, up to $A_V \sim 25$ mag. Figure 2 shows that X-ray emission is preferentially detected from the BDs with relatively low extinction: the detection fraction is $7/16 = 44\%$ for the BDs with $A_V \leq 5$ mag but only $2/18 = 11\%$ for the BDs with $A_V > 5$ mag.

4. TEMPORAL AND SPECTRAL X-RAY CHARACTERISTICS OF THE BROWN DWARFS

Due to the intrinsic X-ray faintness of substellar objects, most previous X-ray observations of BDs have yielded only very small numbers of photons, often too few to allow a reasonable spectral or temporal analysis. Even the extraordinary deep exposure of the COUP data set yields only moderate numbers ($\lesssim 100$) of source photons for the X-ray–detected BDs in the ONC. Nevertheless, these are enough to allow us to retrieve important information from the X-ray data.

4.1. *Light Curve Analysis*

Figure 3 shows the light curves of the X-ray–detected BDs. All objects show evidence for rather strong variability; in most cases, flarelike bursts are seen. In order to characterize the variability in an objective way, the maximum-likelihood blocks (MLBs) algorithm has been used, which segments the light curve into a contiguous sequence of constant count rates (for a full description of the method, see Wolk et al. 2005); this makes it possible to determine the number of flares and the characteristic level of X-ray emission objectively. The MLB algorithm is similar to the Bayesian block analysis, the application of which to the COUP data is described in Getman et al. (2005a), but attempts to overcome one of the limitations of the latter technique, namely that it is able to segment a light curve into only two segments at a time. This appears to be a drawback in the search for faint impulsive events (e.g., flares), as a two-segment representation of the light curve in which one segment includes the event, might not be statistically significant, preventing the segmentation process from starting. Here we are mainly interested in the number of flares and in the characteristic count rate, which can be seen as an estimate of the "quiescent" level of X-ray emission, as opposed to the average count rate, which simply includes all X-ray counts measured, whether in or out of a flare. We note that the meaning of "quiescent" X-ray emission is not clear; for example, apparently quiescent emission may, in reality, just be a superposition of numerous unresolved flares. Nevertheless, the characteristic level can be taken to describe the "usual" X-ray output of the source, outside periods of strong flares. The results of the MLB analysis are listed in Table 4.

We first consider the flares in the X-ray light curves of the BDs. The total number of flares identified by the MLB algorithm in the nine light curves is 13, which corresponds to a flare rate of about one flare per object per 180 hr, consistent with the flare rate of one per 200 hr derived for a sample of 28 solar-like stars in COUP by Wolk et al. (2005). In this regard at least, the temporal characteristics of the X-ray emission from the BDs therefore appear to be quite similar to those of low-mass stars in the ONC.

The second important result from the MLB analysis of the light curves is that a characteristic level could be definitively established for all spectroscopic BDs with the exceptions of COUP 344 (HC 722), which was detected only during a flare and which will be discussed in more detail in § 4.2, and COUP 941 (HC 594), where it was measured at less than 3 σ significance. For the other BDs, however, the characteristic level is clearly established and demonstrates that these objects would have been detected as X-ray sources even without the flares. It also implies that the sources do tend to produce X-ray emission in a more continuous manner than just during occasional large flares. The detection of apparently "quiescent" emission from these BDs is important with respect to the origin of the emission, as discussed further in § 6.

The characteristic count rates are also used to compute an estimate for the characteristic X-ray luminosity by multiplying the temporally averaged X-ray luminosity, as determined from the spectral analysis, by the ratio of the characteristic count rate to the mean count rate over the COUP exposure. We note that this scaling of the luminosities is not fully self-consistent, because the X-ray spectral parameters (e.g., plasma temperatures) may change as a function of the emission level, whereas the X-ray luminosity was determined from the fits to the full, temporally averaged spectra. A fully self-consistent determination of the characteristic X-ray luminosities would require time-resolved spectroscopic analysis, but due to the low number of detected source counts per BD, this is not possible.

Comparison with the pre-COUP X-ray observations of the ONC provides an opportunity to look for long-term variability of the X-ray sources. Four of the X-ray–detected BDs (COUP 280, 371, 1125, and 1313) were detected as X-ray sources in the previous 23 hr *Chandra* ACIS-I observation discussed by Feigelson et al. (2002a). The 23 hr observation light curves of all four sources were classified as "constant" and their reported X-ray luminosities are generally quite consistent with those derived from the COUP data to within a factor of ~ 2–3: the only exception is COUP 371 (HC 90), for which a ~ 6 times higher luminosity was derived from the 23 hr observation than found here from the COUP data.

Most of the COUP detected BDs that remained undetected in the 23 hr observation yielded fewer than 50 counts in the 233 hr COUP data set, giving a consistent low level of X-ray emission. Conversely, one source in the earlier data set, CXO ONC 053518.2−052346, coincides with an SHC04 BD, HC 221 (spectral type M7.5), which was undetected in COUP. Fourteen counts were detected giving $\log L_t \sim 28.5$ in the earlier observation, and no evidence for variability was reported. Using PIMMS, we estimate an extinction-corrected X-ray luminosity of $\log L_X \sim 29.0$ ergs s^{-1}, yielding a fractional X-ray luminosity of $\log (L_X/L_{bol}) \sim -3.1$ for HC 221. The upper limit derived from the COUP data is a factor of about 4 lower than the X-ray luminosity measured in the 23 hr observation.

These comparisons suggest that the level of activity in most of the BDs did not change dramatically over the several years between 1999 October/2000 April when the 23 hr observation was obtained and 2003 January when the COUP observations
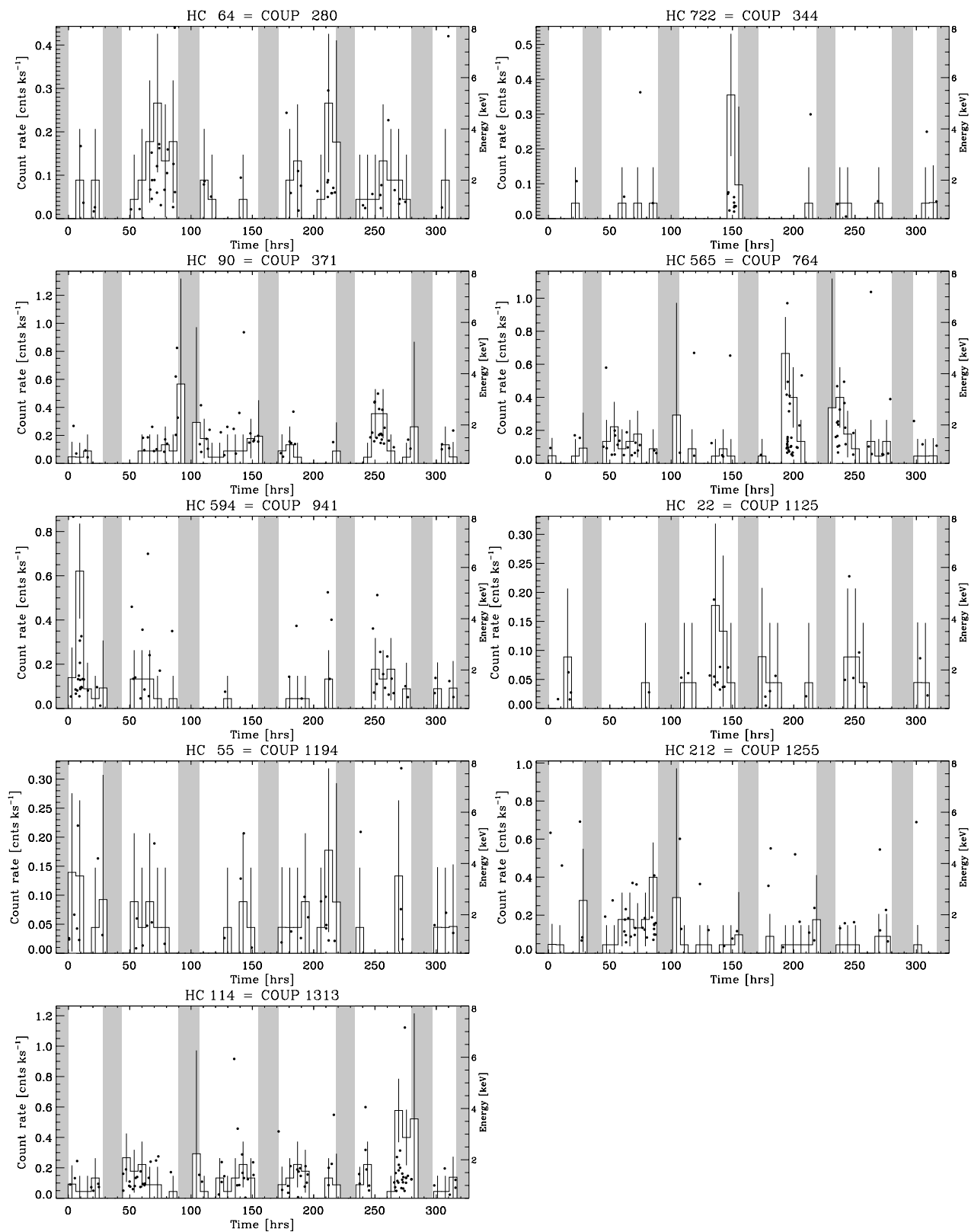
FIG. 3.—Histogram representation of the light curves of the nine X-ray–detected spectroscopic BDs from SHC04 in the [0.5–8] keV band. The filled dots mark the energies and arrival times of the individual photons in each source area. The gray stripes mark the time periods when *Chandra* was not observing.

COUP Number	HC	Average Count Rate (counts ks^{-1})	Characteristic Count Rate (counts ks^{-1})	Number of Flares
280.....................	64	0.058	0.035	2
344.....................	722	0.012	<0.006	1
371.....................	90	0.074	0.028	2
764.....................	565	0.077	0.033	2
941[a]	594	0.051	0.008	2
1125...................	22	0.031	0.022	1
1194...................	55	0.029	0.029	0
1255...................	212	0.054	0.035	1
1313...................	114	0.111	0.090	1

[a] In COUP 941, the characteristic count rate is below the 3 σ limit.

took place. There is evidence for changes by more than a factor of ∼4 in just two sources.

4.2. *The X-Ray Flare on COUP 344 (HC 722)*

The object COUP 344 (HC 722) deserves special attention since it was only detected during an X-ray flare. As noted above, HC 722 is the only COUP-detected object in the SHC04 sample for which a high gravity was found from the spectral analysis, rather than a low gravity as seen for almost all other young members of the ONC. This finding and the extinction estimate of $A_V = 0$ mag tend to imply that COUP 344 is not a member of the ONC, but that it is more likely to be an older, foreground field source. Keeping in mind the revised M6–M6.5 spectral type and $T_{\rm eff} = 2720$ K for COUP 344 as mentioned above, and assuming that COUP 344 is 1 Gyr rather than 1 Myr old, it would have a mass of ∼0.095 $M_\odot$ (i.e., it would be a star and not a BD) and lie at a distance ∼330 pc with time-averaged X-ray luminosity log $L_X \sim 27.3$.

Whether or not the object is a member of the ONC, the time-averaged X-ray luminosity is a poor representation of its flaring behavior. Eight of the 18 counts detected from COUP 344 outside the 9 hr flare are consistent with the measured background rate. Adopting an upper limit of 5 true source photons during this period gives a limit to the quiescent emission of log $L_{X,q} < 27.1$ ergs s^{-1} with log $\left(L_{X,q}/L_{\rm bol}\right) < -3.6$. During the flare, 8 counts arrived of which none are likely to be background. The flare luminosity averaged over this 9 hr period is $L_{X,q} \simeq 28.7$ ergs s^{-1} with log $\left(L_{X,f}/L_{\rm bol}\right) \simeq -2.0$.

4.3. *X-Ray Spectra and Plasma Temperature*

The COUP spectra of the BDs (with the exception of COUP 344, which has only 10 net source counts) were fitted with single-temperature plasma models; a two-temperature model was required only for COUP 280 (HC 64) to yield an adequate fit to its spectrum. Given the rather small numbers (<100) of counts per spectrum, the spectral fit parameters (plasma temperatures and absorbing hydrogen column densities) are subject to relatively large uncertainties. Rather than considering the plasma temperatures derived in the fits, we will therefore only consider the median energy of the COUP-detected X-ray photons (Table 2), which can (for sources with low extinction, $A_V \lesssim 5$ mag) be regarded as a proxy for the plasma temperature. Figure 4 compares the median photon energies of the BDs to those of low-mass stars from the COUP optical sample
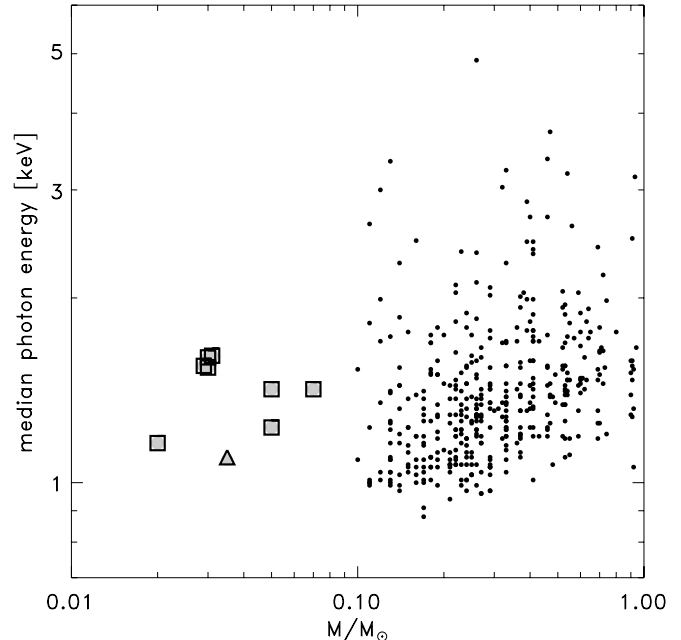

Fig. 4.—Median photon energy vs. mass for the COUP-detected BDs [*gray filled squares*; the triangle shows COUP 344 (HC 722), which was only detected during a flare] and low-mass stars with low optical extinction ($A_V \leq 5$ mag) from the COUP optical sample (*filled circles*; Preibisch et al. 2005).

(Preibisch et al. 2005): the median photon energies of the BDs are seen to be generally similar to those of the low-mass stars. The outlier in this plot is the rather low median-energy value found for COUP 344. Given that this object was detected only during a flare, it appears that its X-ray emission is unusually soft in comparison to that seen from flaring low-mass stars.

5. X-RAY PROPERTIES OF THE BROWN DWARFS COMPARED TO LOW-MASS ONC STARS

To put the observed X-ray properties of the detected BDs into context, we can compare them with those of the X-ray–emitting low-mass stars in the ONC. Preibisch et al. (2005) define a "COUP optical sample" for the purpose of investigating relations between the X-ray properties and other stellar properties of T Tauri stars in the ONC. The COUP optical sample is a well-defined, homogenous, and representative sample of comprehensively characterized young stars and extends down to objects with spectral types of M6.5 with estimated masses around 0.1 $M_\odot$. Nearly all objects in the COUP optical sample are safely classified as stars regardless of the tracks that are used (e.g., have spectral types ≲ M5).

The SHC04 sample includes stellar-mass sources in addition to the BDs, but although there is some overlap in mass with the COUP optical sample, it is important to note that the two samples cannot be easily quantitatively compared for several reasons. First, the COUP optical sample is based on a magnitude-limited ($I < 17.5$) sample of ONC stars from Hillenbrand (1997), whereas the SHC04 sample consists of mostly much fainter sources that were selected as BD candidates from near-infrared photometry. The BD candidate selection criteria include a nominal upper limit brightness of $K \gtrsim 14$, but also some randomly selected brighter objects. As a consequence, the two samples cannot be considered equally complete. Second, the SHC04 sample covers a much smaller area than the COUP optical sample, thus leading to poorer statistics. Third, SHC04 used the D'Antona & Mazzitelli (1997) evolutionary models to
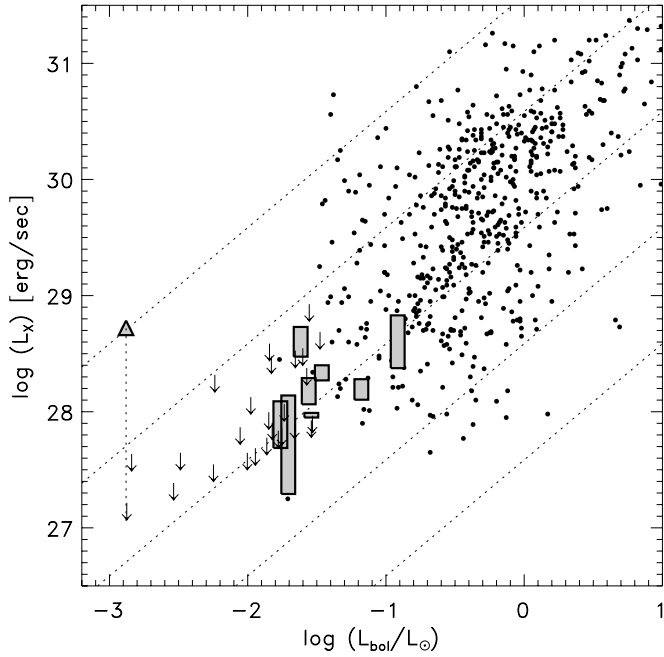
FIG. 5.—X-ray luminosity vs. bolometric luminosity for the BDs from SHC04 (*gray filled boxes; arrows for upper limits*) and low-mass stars from the COUP optical sample (*filled circles*). The gray filled boxes for the BDs extend from the characteristic X-ray luminosity found with the MLB analysis (*lower edge of the box*) to the average X-ray luminosity (*upper edge of the box*). For COUP 344 (HC 722), we show the X-ray luminosity during the flare (*gray filled triangle*) and the upper limit to the quiescent emission level (*arrow*). Some of the symbols have been slightly shifted along the x-axis to avoid overlaps. The dotted lines mark L_X/L_{bol} ratios of 10^{-2}, 10^{-3}, 10^{-4}, 10^{-5}, and 10^{-6}.

estimate masses for their sample, whereas the masses of the COUP optical sample have been estimated using the models of Siess et al. (2000). These latter tracks were adopted as a COUP policy on the basis that they extend across the full mass range encountered in the ONC stellar population, yielding a more uniform approach to intercomparing stellar properties (Preibisch et al. 2005). They do not, however, extend into the BD mass domain, making it impossible to use them in the present paper. With these caveats in mind, it is nevertheless instructive to compare the properties of the spectroscopic BDs of SHC04 with those of the low-mass stars from the COUP optical sample in at least a qualitative way.

Figure 5 shows the distribution of X-ray versus bolometric luminosities for the BDs and low-mass stars in the ONC. Considering only the X-ray–detected BDs, the fractional X-ray luminosities lie in the range $\log(L_X/L_{bol}) \sim -4$ to -3, similar to that seen for the low-mass stars. Excluding COUP 344 (HC 722), which was only detected during a large flare, the median fractional X-ray luminosity of the 8 remaining X-ray–detected BDs is $\log(L_X/L_{bol}) = -3.76$, which is identical to the median fractional X-ray luminosity of the X-ray–detected $0.1-0.25$ $M_\odot$ stars in the COUP optical sample. Considering the upper limits for undetected BDs as well, we find an upper limit for the median fractional X-ray luminosity of $\log(L_X/L_{bol}) < -3.8$; this is only marginally lower than the median value for the detected BDs because most of the undetected BDs are seen through more extinction than the X-ray–detected BDs (see § 3.6), and therefore most upper limits to the extinction-corrected X-ray fluxes are essentially at the same level as the fluxes for the detected BDs.

Investigating this effect further, Figure 6 shows the fractional X-ray luminosity $[\log(L_X/L_{bol})]$ versus mass for the SHC04
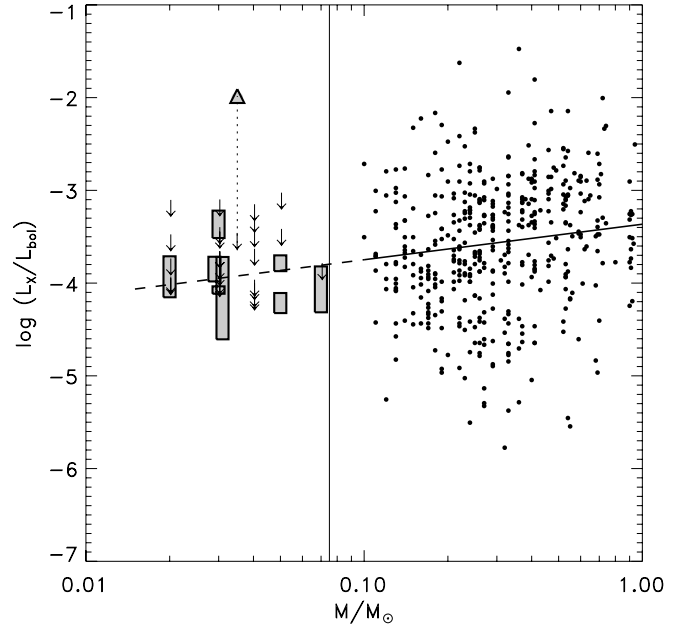

FIG. 6.—Fractional X-ray luminosity $\log(L_X/L_{bol})$ vs. mass for BDs from the SHC04 sample and low-mass stars from the COUP optical sample. The symbols are as in Fig. 5. The solid line shows a linear regression fit to the low-mass ($0.1-2$ $M_\odot$) stars, while the dashed line shows the same fit extrapolated into the BD regime.

BDs and low-mass stars from the COUP optical sample. A regression fit derived in Preibisch et al. (2005) for the low-mass ($0.1-2$ $M_\odot$) stars is plotted, along with an extrapolation of this fit into the BD regime. The BDs seem to follow this extrapolation, in the sense that the fractional X-ray luminosity continues to decrease slightly in going from low-mass stars to BDs. As discussed in § 3.2, it is possible that the use of near-infrared classifications and a field dwarf effective temperature scale by
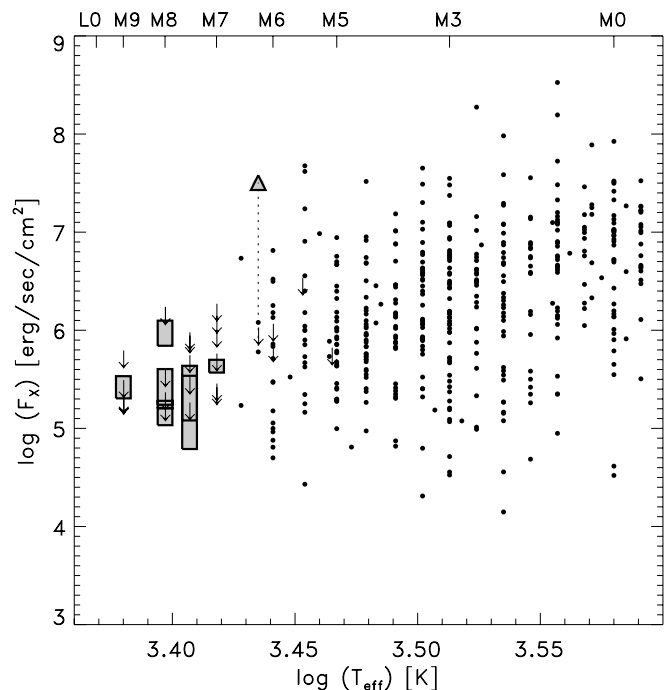

FIG. 7.—X-ray surface flux vs. effective temperature for the SHC04 BDs and low-mass stars from the COUP optical sample. The symbols are as in Fig. 5.
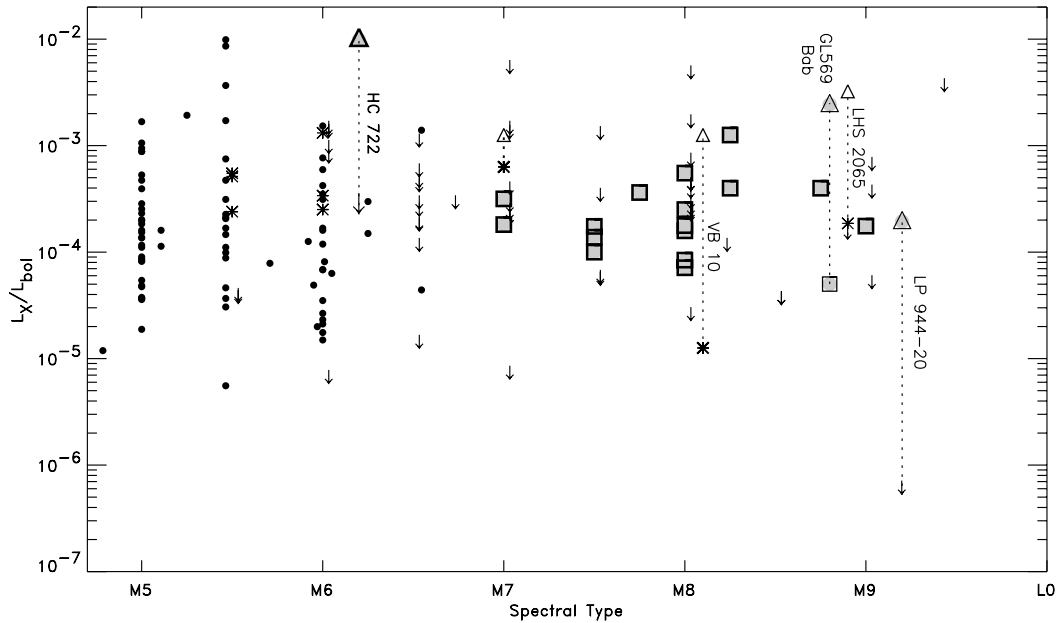
FIG. 8.—Fractional X-ray luminosity vs. spectral type for objects of type M5 or later. The filled circles show stars in the COUP optical sample. Data for late M field stars from Fleming et al. (1993) are shown as asterisks (*). The BDs in the ONC from the SHC04 sample and other X-ray–detected young BDs (as discussed in § 2) are shown by gray filled squares. For objects with strong flares, the values at flare peak are shown by triangles, connected by dotted lines to the quiescent emission values (or upper limits). Some individual objects discussed in the text are annotated. Some symbols have been slightly shifted along the x-axis to avoid overlaps.

SHC04 have led to a systematic underestimate of the masses in their sample by a factor of up to 2−3. If so, this would push them somewhat to the right in Figure 6 but would not greatly affect the general agreement with the extrapolated trend from the low-mass stars with optical spectral types.

In Figure 7 we show a plot of the X-ray surface flux (i.e., the X-ray luminosity divided by the surface area of the object, which is computed from its bolometric luminosity and effective temperature) versus the effective temperature for the SHC04 BDs and the COUP optical sample of low-mass stars. Here the variables are more directly measurable than the mass, which may be affected by uncertainties in the theoretical models as previously discussed. Our data show that the BDs follow the general trend of decreasing surface fluxes with decreasing effective temperature. The mean surface fluxes in the coronae of the BDs are more than 1 order of magnitude lower than those in early M-type stars, although they are still about 1 order of magnitude higher than the typical average X-ray surface flux in the solar corona.

Again, these deductions would not be significantly affected if the true effective temperatures of the BD sample were larger than those derived by SHC04. An increase in effective temperature by 300 K would result in a source moving by ∼0.06 dex to the right in Figure 7 and by ∼0.2 dex up, as the surface flux is the X-ray luminosity divided by the area of the source, and the area scales as $T_{\rm eff}^{-4}$ for constant bolometric luminosity. It can be readily seen in Figure 7 that the source would still remain well within the extrapolation from the COUP optical sample.

6. DISCUSSION: ON THE ORIGIN OF STELLAR AND SUBSTELLAR X-RAY EMISSION

We now consider the implications of our findings on astrophysical concepts underlying the production of magnetic activity on BD surfaces. In solar-type main-sequence stars, the differentiated radiative and convective inner structure leads to an $\alpha-\Omega$ dynamo, which in turn generates magnetic fields that can sustain a hot corona where X-rays can be emitted. However,

both low-mass pre–main-sequence stars and BDs are fully convective, and thus it remains unknown how magnetic fields may arise in them. Potential alternative dynamo mechanisms are small-scale dynamo action in a highly turbulent convection zone (cf. Durney et al. 1993; Giampapa et al. 1996 and references therein) or a so-called α^2 dynamo, as suggested by Küker & Rüdiger (1999). A more detailed discussion can be found in Feigelson et al. (2003).

Figure 8 shows the fractional X-ray luminosities as a function of spectral type for the coolest objects in the ONC and compares them to equivalent data obtained for other very cool objects. It confirms that very young ONC BDs with spectral types in the range M6–M9 show essentially the same signatures of activity as older, low-mass field stars and BDs with equivalent late-M spectral types. The implication is that the activity is mainly determined by the effective temperatures of the sources and not (so much) by their masses, since the ONC BDs are typically a factor of 4 or so lower in mass than field dwarfs of the same spectral type (Baraffe et al. 1998). Similarly, the substantial difference in surface gravity (∼30 times higher in an M8 field star compared to an M8 1 Myr old BD) appears not to be important. Finally, the main difference between BDs and stars, i.e., the presence or absence of nuclear hydrogen burning, seems not to play a role in the X-ray activity. This latter finding is not very surprising, as it has been known for many years that low-mass pre–main-sequence stars, which have not yet started nuclear fusion processes, are generally strong X-ray sources.

The key to understanding the X-ray activity of very young BDs seems to be that they have relatively early spectral types of M6–M9 for their mass and are thus still warm enough to maintain a partially ionized atmosphere. As the photospheric properties of these young substellar objects are essentially the same as those of older stellar objects, it is not surprising that their coronal properties are similar to those of low-mass stars. In other words, the very young BDs do not yet know that they will never undergo hydrogen fusion, and therefore they behave like low-mass stars.

While X-ray emission is now clearly established for very cool dwarfs down to spectral type M9, no X-ray detections of L- or T-type objects have been reported to date, again keeping in mind that COUP 344/HC 722 has been reclassified from L0 to M6–M6.5. It is unclear whether the nature of the X-ray emission changes at or beyond spectral type ∼M9, or whether the few available X-ray data points on cooler objects are just not sensitive enough to provide useful constraints. Observations of very cool field objects have provided some indications of changes in the X-ray properties among the coolest X-ray–detected objects (§ 2). The ∼M9 objects LHS 2065 (Schmitt & Liefke 2002; note that LHS 2065 is a very-low mass star and not a BD), Gl 569 Ba, b (Stelzer 2004), and LP 944-20 (Rutledge et al. 2000) showed X-ray flares, but no fully convincing evidence of continuous ("quiescent") X-ray emission was found. In particular, the very restrictive upper limit to possible quiescent emission from the field BD LP 944-20 [$\log (L_X/L_{bol}) < -6.3$] found by Martín & Bouy (2002) supported the idea that the coolest X-ray–detected objects may emit X-rays only during flares, unlike the earlier M dwarfs for which some kind of quiescent emission has clearly been established.

Our detection of apparently quiescent X-ray emission from the ONC BD HC 212 is relevant in this context. Its near-infrared spectral type is M9, although again, it is possible that its optical spectral type would be earlier. Nevertheless, taken at face value, it would appear to demonstrate that at least young M9 objects can produce not only X-ray flares, but also more steady X-ray emission. This finding is supported by the detection of probably quiescent X-ray emission from the young (∼10 Myr) TWA-5B by Tsuboi et al. (2003), which has an optical spectral type of M8.5–M9 (Neuhäuser et al. 1999). Thus, it appears as though quiescent emission may indeed by possible at a spectral type of M9 when the source is young, although it remains unclear whether this is only because young M9 sources may be significantly warmer than their field star counterparts, as discussed above in § 3.2.

Another important result in this context is the observed drop in the typical X-ray surface fluxes by about 1 order of magnitude between early and late M spectral types (Fig. 7); this suggests that the coronal properties of very cool stars do indeed change over the temperature range ∼3700 to ∼2400 K. Mohanty & Basri (2003) noted an analogous change in the chromospheric properties, as traced by $F_{H\alpha}$ and $L_{H\alpha}/L_{bol}$, over a similar spectral type range (M4–M9) in field stars.

Finally, we note that strong changes in the coronal properties are expected across the M- to L-type transition from observational indications as well as from theoretical considerations. Observational evidence comes from the sharp and strong drop in Hα emission (a tracer of chromospheric activity) around spectral type M9–L0 for field dwarfs (Gizis et al. 2000; Mohanty & Basri 2003). The lack of chromospheric activity in the ultracool L-type dwarfs is most likely related to the fact that the atmospheres of objects cooler than $T_{eff} \sim 2400$ K (corresponding to spectral type M9) are essentially neutral and have a very high electrical resistivity, in which the rapid decay of currents prevents the buildup of magnetic free energy and therefore cannot provide support for magnetically heated chromospheres and coronae (see Fleming et al. 2000; Mohanty et al. 2002). These ultracool dwarfs should therefore not produce the same kind of quiescent X-ray emission as originates from magnetically confined plasma in the coronae of late-type stars. However, it is interesting to note that several studies have found flaring Hα emission in some L- and T-type dwarfs (e.g., Burgasser et al. 2000; Hall 2002; Liebert et al. 2003). These discoveries suggest that even the ultracool dwarfs can show some kind of magnetic activity, although it probably has a different nature to that seen in the hotter M-type dwarfs. One possible explanation is that rapidly rising individual flux tubes from the interior of these objects dissipate currents in the atmosphere and cause flares (Mohanty et al. 2002).

7. CONCLUSIONS

The data of the *Chandra* Orion Ultradeep Project have provided X-ray detections for 9 of the 34 spectroscopically confirmed BDs of SHC04 in the central part of the Orion Nebula Cluster. The low detection fraction is not only related to the intrinsic faintness of these objects, but also to the foreground extinction, which is, in many cases, substantial. Considering only the BDs with $A_V \leq 5$ mag, the detection fraction is 7/16 = 44%. For all but one of the X-ray–detected late M-type BDs, an analysis of their X-ray light curves revealed evidence for continuous ("quiescent") emission in addition to several large flares. Our results extend the spectral type of the coolest known object with clear evidence for quiescent X-ray emission down to M9, although we note that corresponding spectral type was obtained via near-infrared spectroscopy and should be confirmed via optical spectroscopy if possible.

Our results show no evidence that BDs with ages around 1 Myr are significantly less magnetically active than late-type stars of similar ages. A gradual trend of decreasing fractional X-ray luminosity or X-ray surface flux is seen as one progresses from 1 to 0.1 $M_\odot$ to BD masses, but no sharp change in X-ray properties at the substellar boundary is seen. The X-rays are seen in both flare and apparently quiescent modes. These results are consistent with previous *Chandra* studies of young BDs in nearby star-forming regions, although these involved smaller samples and shorter exposures.

A comparison of the X-ray properties of the late M-type BDs with those of late-type stars suggests that they share a common X-ray emission mechanism that is governed primarily by the photospheric temperature, not by the mass or surface gravity of the source. The absence of any clear transition in X-ray properties across the stellar/substellar mass boundary implies that this conclusion is robust against uncertainties in the detailed classification of sources on either side of that boundary.

REFERENCES

Baraffe, I., Chabrier, G., Allard, F., & Hauschildt, P. H. 1998, A&A, 337, 403
Basri, G. 2000, ARA&A, 38, 485
Burgasser, A. J., Kirkpatrick, D., Reid, I. N., Liebert, J., Gizis, J. E., & Brown, M. E. 2000, AJ, 120, 473
Comerón, F., Neuhäuser, R., & Kaas, A. A. 2000, A&A, 359, 269
D'Antona, F., & Mazzitelli, I. 1997, Mem. Soc. Astron. Italiana, 68, 807
Durney, B. R., De Young, D. S., & Roxburgh, I. W. 1993, Sol. Phys., 145, 207
Feigelson, E. D., & Lawson., W. A. 2004, ApJ, 614, 267

Feigelson, E. D., Broos, P., Gaffney, J. A., Garmire, G., Hillenbrand, L. A., Pravdo, S. H., Townsley, L., & Tsuboi, Y. 2002a, ApJ, 574, 258

Feigelson, E. D., Garmire, G. P., & Pravdo, S. H. 2002b, ApJ, 572, 335

———. 2003, ApJ, 584, 911

Flaccomio, E., et al. 2003a, ApJ, 582, 382

———. 2003b, ApJ, 582, 398

Fleming, T. A., Giampapa, M. S., & Schmitt, J. H. M. M. 2000, ApJ, 533, 372

Fleming, T. A., Giampapa, M. S., Schmitt, J. H. M. M., & Bookbinder, J. A. 1993, ApJ, 410, 387

Garmire, G., Feigelson, E. D., Broos, P., Hillenbrand, L. A., Pravdo, S. H., Townsley, L., & Tsuboi, Y. 2000, AJ, 120, 1426

Getman, K. V., et al. 2005a, ApJS, 160, 319

———. 2005b, ApJS, 160, 353

Giampapa, M. S., Rosner, R., Kashyap, V., Fleming, T. A., Schmitt, J. H. M. M., & Bookbinder, J. A. 1996, ApJ, 463, 707

Gizis, J. E., & Bharat, R. 2004, ApJ, 608, L113

Gizis, J. E., et al. 2000, AJ, 120, 1085

Gorlova, N. I., Meyer, M. R., Rieke, G. H., & Liebert, J. 2003, ApJ, 593, 1074

Hall, P. B. 2002, ApJ, 564, L89

Herbst, W., Bailer-Jones, C. A. L., Mundt, R., Meisenheimer, K., & Wackermann, R. 2002, A&A, 396, 513

Hillenbrand, L. A. 1997, AJ, 113, 1733

Hillenbrand, L. A., & Carpenter, J. M. 2000, ApJ, 540, 236

Hillenbrand, L. A., & White, R. J. 2004, ApJ, 604, 741

Imanishi, K., Tsujimoto, M., & Koyama, K. 2001, ApJ, 563, 361

Küker, M., & Rüdiger, G. 1999, A&A, 346, 922

Liebert, J., et al. 2003, AJ, 125, 343

Lucas, P. W., & Roche, P. F. 2000, MNRAS, 314, 858

Lucas, P. W., Roche, P. F., Allard, F., & Hauschildt, P. H. 2001, MNRAS, 326, 695

Luhman, K. L. 1999, ApJ, 525, 466

Luhman, K. L., & Reike, G. H. 1999, ApJ, 525, 440

Luhman, K. L., Stauffer, J. R., Muench, A. A., Rieke, G. H., Lada, E. A., Bouvier, J., & Lada, C. J. 2003, ApJ, 593, 1093

Luhman, K. L., et al. 2000, ApJ, 540, 1016

Martín, E. L., & Bouy, H. 2002, NewA, 7, 595

McCaughrean, M. J., Zinnecker, H., Rayner, J. T., & Stauffer, J. R. 1995, in The Bottom of the Main Sequence—and Beyond, ed. C. G. Tinney (Heidelberg: Springer), 209

McGovern, M. R., Kirkpatrick, J. D., McLean, I. S., Burgasser, A. J., Prato, L., & Lowrance, P. J. 2004, ApJ, 600, 1020

Mohanty, S., & Basri, G. 2003, ApJ, 583, 451

Mohanty, S., Basri, G., Shu, F., Allard, F., & Chabrier, G. 2002, ApJ, 571, 469

Muench, A. A., Lada, E. A., Lada, C. J., & Alves, J. 2002, ApJ, 573, 366

Neuhäuser, R., & Comerón, F. 1998, Science, 282, 83

Neuhäuser, R., et al. 1999, A&A, 343, 883

Ozawa, H., Grosso, N., & Montmerle, T. 2005, A&A, 429, 963

Preibisch, Th., & Zinnecker, H. 2001, AJ, 122, 866

———. 2002, AJ, 123, 1613

Preibisch, Th., et al. 2005, ApJS, 160, 401

Rutledge, R. E., Basri, G., Martín, E. L., & Bildsten, L. 2000, ApJ, 538, L141

Schmitt, J. H. M. M., & Liefke, C. 2002, A&A, 382, L9

Siess, L., Dufour, E., & Forestini, M. 2000, A&A, 358, 593

Slesnick, C. L., Hillenbrand, L. A., & Carpenter, J. M. 2004, ApJ, 610, 1045 (erratum, 625, 1063 [2005]) (SHC04)

Stelzer, B. 2004, ApJ, 615, L153

Stelzer, B., Micela, G., & Neuhäuser, R. 2004, A&A, 423, 1029

Tsuboi, Y., et al. 2003, ApJ, 587, L51

Vuong, M. H., Montmerle, T., Grosso, N., Feigelson, E. D., Verstraete, L., & Ozawa, H. 2003, A&A, 408, 581

White, R. J., Ghez, A. M., Reid, I. N., Schultz, G. 1999, ApJ, 520, 811

Wilking, B. A., Meyer, M. R., Greene, T. P., Mikhail, A., Carlson, G. 2004, AJ, 127, 1131

Wolk, S. J., et al. 2005, ApJS, 160, 423

Zapatero Osorio, M. R., Pavlenko, Y., Martín, E. L., Britton, M., & Kulkarni, S. R. 2004, ApJ, 615, 958